Supplementary Information

Chemicals and materials:

Ti_3AlC_2 powder (400 mesh, purchased from 11 Technology Co. Ltd.), sodium hydroxide (NaOH, Macklin, ≥97.0%), tetramethylammonium hydroxide ($C_4H_{13}NO$, Aladdin, 25 wt%), dimethyl sulfoxide (C_2H_6OS, Aladdin, ≥99.8%), sodium hypochlorite solution (NaClO, Energy Chemical, 14.5 wt%), hydrochloric acid (HCl, General reagent, 36-38 wt%), salicylic acid ($C_7H_6O_3$, Macklin, ≥99.5%), sodium citrate dehydrate ($C_6H_5Na_3O_7.2H_2O$, Aladdin, ≥99.0%), sodium pentacyanonitrosylferrate dehydrate ($C_5FeN_6Na_2O{\cdot}2H_2O$, Alfa Aesar, ≥98.0%), p-dimethylaminobenzaldehyde ($C_9H_{11}NO$, Aladdin, ≥99.0%), ethanol absolute (C_2H_6O, Sinopharm Chemical Reagent Co. Ltd, ≥99.8%), N, N-Dimethylformamide (C_3H_7NO, Aladdin, ≥99.9%), hydrazine hydrate ($N_2H_4.H_2O$, Alfa Aesar, ≥99.0%), hydrofluoric acid (HF, Aladdin, 40 wt%). N_2 gas (99.99%) and Ar gas (99.99%) were purchased from Shanghai Likang Gas Co. Ltd (Shanghai, China). All chemicals were used as received without further purification.

Preparation of $Ti_3C_2T_x$ (T= O, OH):

$Ti_3C_2T_x$ (T= O, OH) was synthesized according to the paper reported before[1]. About 80 mg Ti_3AlC_2 powder was added into the 35 mL NaOH solution (27.5 M) contained in a 50 mL autoclave in argon (Ar) atmosphere. Then the autoclave was heated at 270 °C in an electric thermostatic drying oven for 12 h. Finally, the result suspension was filtered with deionized water washing for several times. The obtained powder was dried at 60 °C for 12 h.

Preparation of $Ti_3C_2T_x$ (T= F, O, OH):

$Ti_3C_2T_x$ (T= F, O, OH) was synthesized according to the paper reported before[2]. 0.5 g Ti_3AlC_2 powder was carefully added to 10 mL HF solution (40 wt%) with stirring for 24 h at 30 °C. Then the product was filtered using a polyvinyl difluoride (PVDF) membrane with 200 nm pore size. The obtained powder was dried at 60 °C for 12 h.

Influence of sodium:

We added a dialysis step to decrease the sodium in NaOH-$Ti_3C_2T_x$ powder after hydrothermal step. $Ti_3C_2T_x$ (T= O, OH) powder was added into a dialysis bag (MW: 5000 Dalton) and then immersed in the deionized water for 2 days. We changed the water every 10 h. Finally, the powder was filtered and washed with deionized water for several times, then dried at 60 °C for 12 h.

Inductive Coupled Plasma Optical Spectrometer (ICP-OS) was used to indicate the element mass ratio before and after dialysis step. The result showed that sodium mass ratio decreased obviously after dialysis treatment (Fig. S11, Na mass ratio: from 8.22% to 3.06%). The resultant sodium may derive from the interlayer of the multilayer NaOH-$Ti_3C_2T_x$, where sodium ions intercalated during the hydrothermal process (See TEM images (Fig. S4) of multilayer NaOH-$Ti_3C_2T_x$ and HF-$Ti_3C_2T_x$, the former has larger layer spacing). The prepared samples were then intercalated and delaminated at the same conditions. The NRR performance showed no obvious difference between the samples achieved with and without dialysis treatment (See Fig. S12). Therefore, sodium does not influence the NRR performance.

Intercalation and delamination:

50 mg $Ti_3C_2T_x$ powder was added into 10 mL tetramethylammonium hydroxide (TMAOH) solution followed by stirring for 24 h. Then $Ti_3C_2T_x$ was separated via centrifugation at 8000 r/min for 20 min. Deionized water was added into the products and then sonication using

ultrasonic processors (600 W) for 6 h in Ar atmosphere. Finally, the smaller sheets were separated via centrifugation at 10000 r/min for 30 min. The process was the same when DMSO was used for the intercalation.

Characterization:

XRD test was conducted using a Rigaku Ultima IV Powder Diffractometer (Cu Kα radiation, sweeping speed: 5 °/min). TEM analysis was performed on a JEM-2100F transmission electron microscope (200 kV, JEOL, Japan). SEM studies were carried out on a Mira3 scanning electron microscope (5 kV for morphology observation, Tescan, Czech). XPS spectra were acquired with a Kratos Axis Ultra^{DLD} spectrometer using a monochromatic Al/K_α source (1486.6 eV). The AFM data were generated from a Bruker multimode 8 operated in ScanAsyst mode. The ratio of Al, Na and Ti were measured with an ICAP7600 inductively coupled plasma optical spectroscopy.

Cathode preparation:

250 μL ethanol and 20 μL Nafion solution were added into 750 μL $Ti_3C_2T_x$ nanosheet solution (~ 2 - 5 mg mL^{-1}) followed by sonication for 30 min to form a homogenous ink. Then the ink was loaded onto a carbon cloth with an area of 0.5 x 0.5 cm^2 (loading: 0.8 mg cm^{-2}) and dried under ambient condition.

Electrochemical NRR measurements:

Before NRR tests, Nafion 117 membrane was heated in a 5% H_2O_2 solution at 80 ℃ for 1 h and deionized water for another 1 h, sequentially. All electrochemical measurements were performed using a traditional three-electrode system with a 0.1 M HCl solution as the electrolyte. $Ti_3C_2T_x$/carbon cloth, carbon rod, and Ag/AgCl in a saturated KCl aqueous solution were used as the working electrode, counter electrode, and reference electrode, respectively. Electrochemical measurements were performed on an electrochemical workstation (Biologic VMP3) with a gas-tight two-compartment electrochemical cell separated by a piece of Nafion 117 membrane. All experiments were performed at ambient conditions (~295 K). For N_2 reduction reaction experiments, the HCl electrolyte (0.1 M) was bubbled with high-purity N_2 (99.99%) for 30 min before measurement. The NRR performance of an electrode was evaluated using controlled potential electrolysis in an electrolyte for 2 h. During each run, the electrolyte was continuously bubbled with N_2 at a flow of ~ 8 sccm, and was agitated with a stirring bar at a stirring rate of ~ 600 rpm. No in-line acid trap was used to capture NH_3 that might escape from the electrolyte in our study and the applied potentials were iR-compensated.

In this paper, E (RHE) = E (Ag/AgCl/saturated KCl) + 0.269 V in 0.1 M HCl. All potentials were referenced to the reversible hydrogen electrode potential in this work. All the polarization curves were the steady-state ones after several cyclic voltammogram (CV) cycles. CV and linear sweep voltammogram (LSV) were performed at a scan rate of 20 mV s^{-1} and 5 mV s^{-1}, respectively. The current density was normalized to the geometric surface area.

Determination of ammonia:

The concentration of NH_3 was determined via indophenol blue method[3]. In detail, 2 mL post-tested solution was removed from the cathode chamber after reaction. Then 2 mL NaOH solution (1 M) containing 5 wt% salicylic acid and 5 wt% sodium citrate was added, followed by 1 mL 0.05 M NaClO and 0.2 mL 1 wt% sodium pentacyanonitrosylferrate dehydrate solution. After 2 h, the absorption spectrum of the mixed solution was detected by an ultraviolet-visible

spectrophotometer. The concentration of NH_3 was determined using the absorbance at the wavelength of 655 nm. The absorbance curves were calibrated using a series of NH_4Cl standard solutions (0.4, 0.8, 1.2, 1.6, 2.0, 2.5, 5.0 μg mL^{-1}, Fig. S7).

Determination of hydrazine:

The concentration of hydrazine in the electrolyte was tested via Watt and Chrisp method[4]. The test kit was composed of p-dimethylaminobenzaldehyde (5.99 g), HCl (concentrated, 30 mL) and ethanol (300 mL). Calibration curves were plotted as follow (Fig. S8): 2 mL color reagent were added into a series of N_2H_4 standard solutions (2 mL, 0, 0.2, 0.4, 0.6, 0.8, 1.0, 2.0 μg mL^{-1}, solvent: HCl). After 15 min, the standard curves can be obtained using absorbance at a wavelength of 455 nm. The concentration of N_2H_4 in electrolyte solution can be easily got when mixed with test kit using the same process.

Calculations of NH_3 yield and Faradaic efficiency:

The NH_3 yield was calculated using the following equation:

$$NH_3 \text{ yield } (\mu g\ h^{-1}\ mg_{cat.}^{-1}) = (c_{NH3} \times V) / (17 \times t \times m)$$

Where c_{NH3} (μg mL^{-1}) is the measured NH_3 concentration; V (mL) is the volume of electrolyte (in our work 40 mL); t (s or h) is the reaction time; m (mg) is the mass loading of catalyst on carbon cloth.

The Faradaic efficiency for NRR was defined as the quantity of electric charge used for synthesizing ammonia and hydrazine hydrate is divided the total charge passed through the electrodes during the electrolysis. Assuming three electrons were needed to produce one NH_3 molecule, The Faradaic efficiency (FE) was calculated according to the following equation:

$$FE = 3F \times C_{NH3} \times V / (17 \times Q) \times 100\%$$

where F is Faraday constant, C_{NH3} is the measured NH_3 concentration, V is the volume of electrolyte, Q is the total charge passed through the electrode.

EIS measurement:

Electrochemical impedance spectroscopy (EIS) measurement (200 kHz to 10 mHz) of NaOH-$Ti_3C_2T_x$ and HF-$Ti_3C_2T_x$ electrodes at -0.3 V versus RHE were conducted using a three-electrode cell with a 1M H_2SO_4 serving as the electrolyte. The result showed that NaOH-$Ti_3C_2T_x$ had a lower ion transport resistance at high frequency (Fig. S13). It can be concluded that fluorine-free property endows NaOH-$Ti_3C_2T_x$ better conductivity.

Electrochemical specific area:

We performed cyclic voltammograms (CV) test to compare the electrochemical specific area of NaOH-$Ti_3C_2T_x$ and HF-$Ti_3C_2T_x$ using a three-electrode cell with a 1 M H_2SO_4 serving as the electrolyte (Fig. S6a and S6b). In the perspective of electrochemistry, $I \propto V * C_s$, where I is steady-state current, V is scanning speed, C_s is a variable related to electrochemical specific area ($C_s \propto$ specific area). Therefore, we conducted CV tests for two electrodes at three different scanning speed (2, 5, 10 mV/s). The mass (m) of the electrodes were also considered. Then we took I / m as Y-axis, V as X-axis and then plotted a straight line and calculated the slope (Fig. S6c and 6d). The result was that HF-$Ti_3C_2T_x$ (K=0.125) had a lower slope than NaOH-$Ti_3C_2T_x$ (K=0.140), meaning a larger specific area of NaOH-$Ti_3C_2T_x$.

Table S1

Catalyst	Electrolyte	NH_3 yield rate	Over-potential	FE	References
Fluorine-Free $Ti_3C_2T_x$/ Carbon cloth	0.1 M HCl	36.9 μg h^{-1} mg_{cat}^{-1}	-0.3 V	9.1%	This work
$Ti_3C_2T_x$/Carbon Paper	0.1 M HCl	20.4 μg h^{-1} mg_{cat}^{-1}	-0.4 V	9.3%	5
$TiO_2/Ti_3C_2T_x$	0.1 M HCl	32.17 μg h^{-1} mg_{cat}^{-1}	-0.55 V	3.2%	6
$Ti_3C_2T_x$ nanosheets attached to a vertically aligned metal host	0.1 M HCl	4.72 μg h^{-1} cm^{-2}	-0.1 V	5.78%	7

Table S2

Intercalation Reagents	NH_3 yield rate	Over-potential	FE
TMAOH	36.9 μg h^{-1} mg_{cat}^{-1}	-0.3 V	9.1%
DMSO	25.4 μg h^{-1} mg_{cat}^{-1}	-0.4 V	9.3%
	18.1 μg h^{-1} mg_{cat}^{-1}	-0.3 V	7.9%
DMF	22.3 μg h^{-1} mg_{cat}^{-1}	-0.4 V	8.6%
	17.4 μg h^{-1} mg_{cat}^{-1}	-0.3 V	7.4%
Ethanol	21.6 μg h^{-1} mg_{cat}^{-1}	-0.4 V	8.4%
	16.6 μg h^{-1} mg_{cat}^{-1}	-0.3 V	6.8%

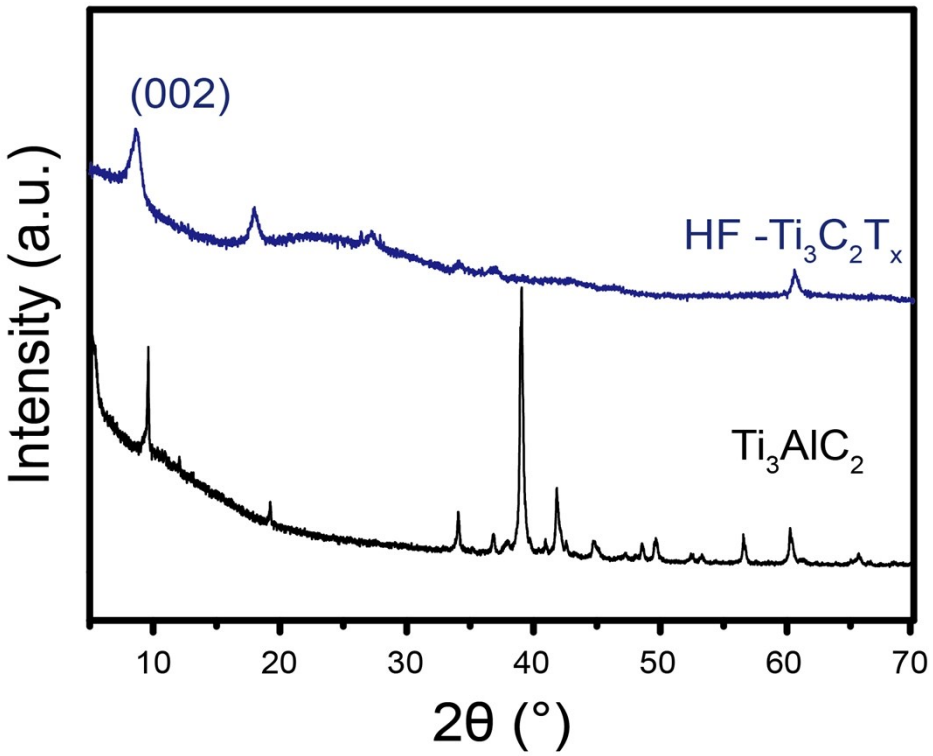

Fig. S1 XRD patterns of Ti_3AlC_2 and $Ti_3C_2T_x$ via HF etching

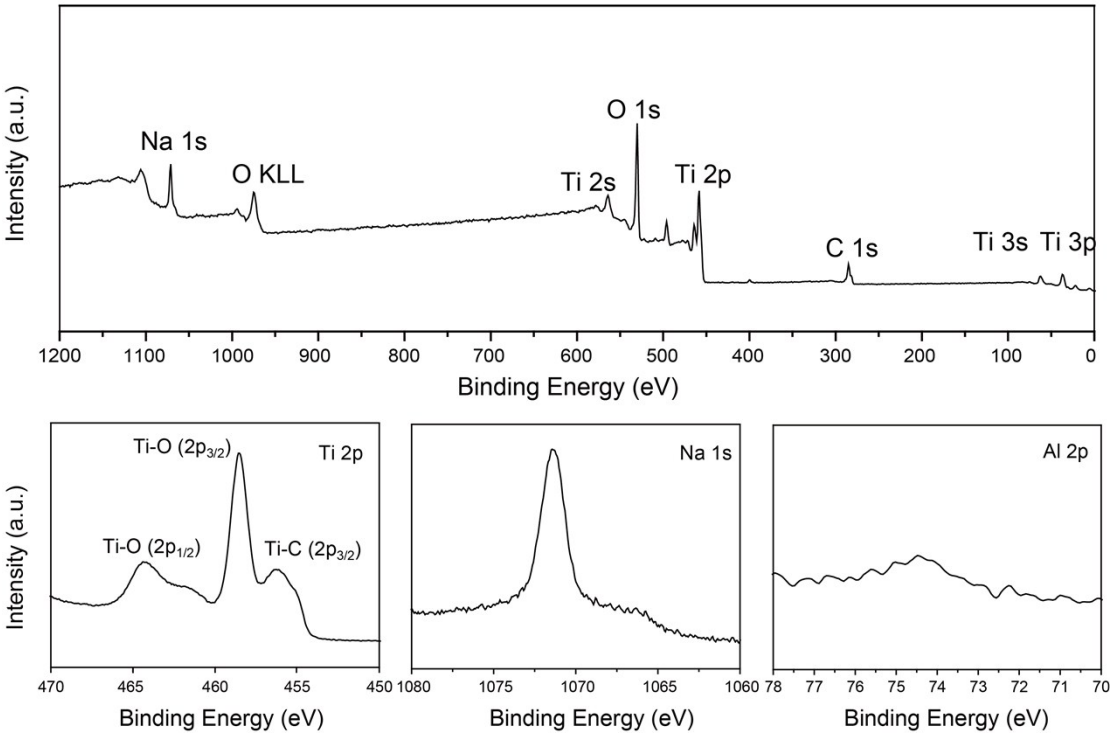

Fig. S2 XPS spectra of the resulting NaOH-$Ti_3C_2T_x$ powder

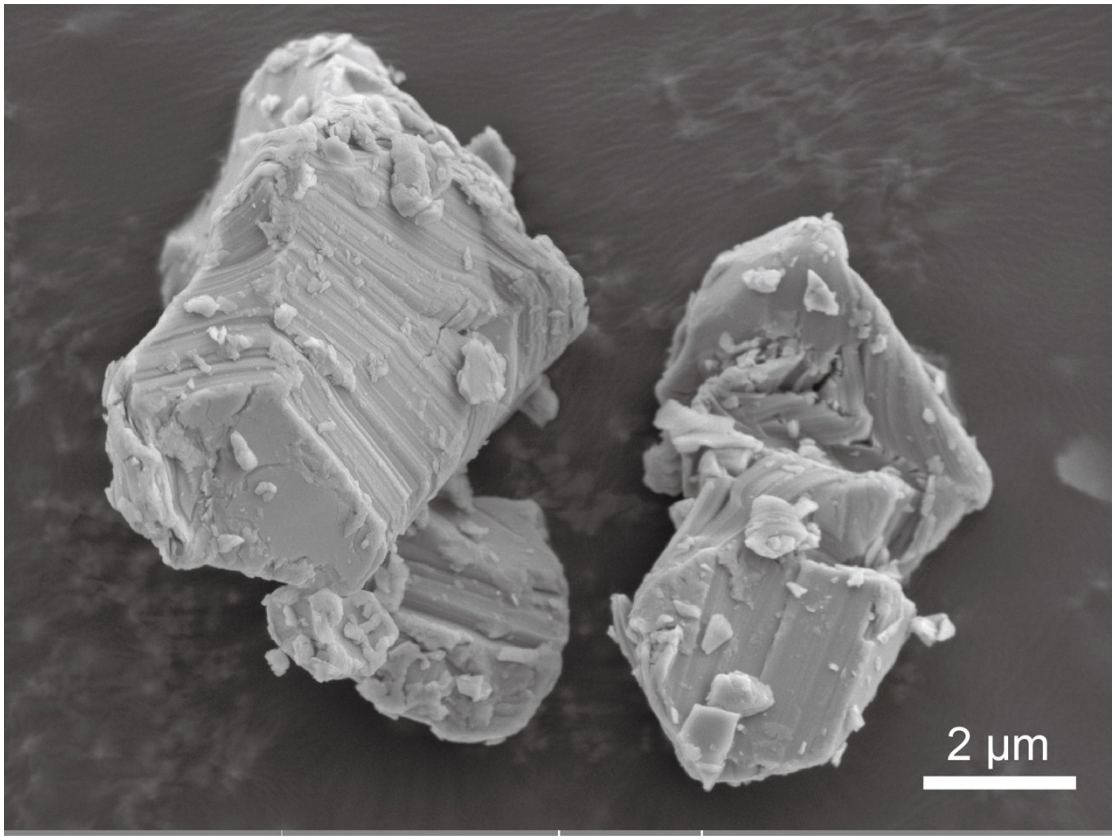

Fig. S3 SEM image of the pristine Ti_3AlC_2 powders

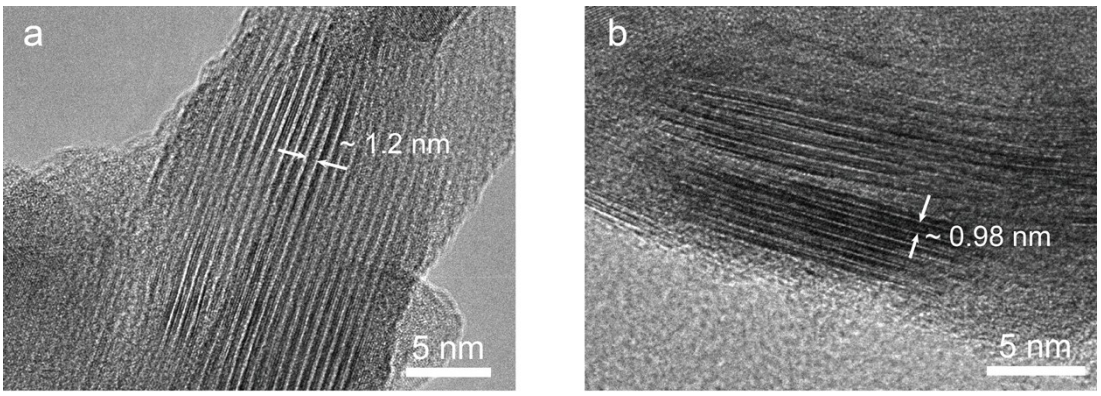

Fig. S4 TEM images of (a) NaOH-$Ti_3C_2T_x$ (b) HF-$Ti_3C_2T_x$

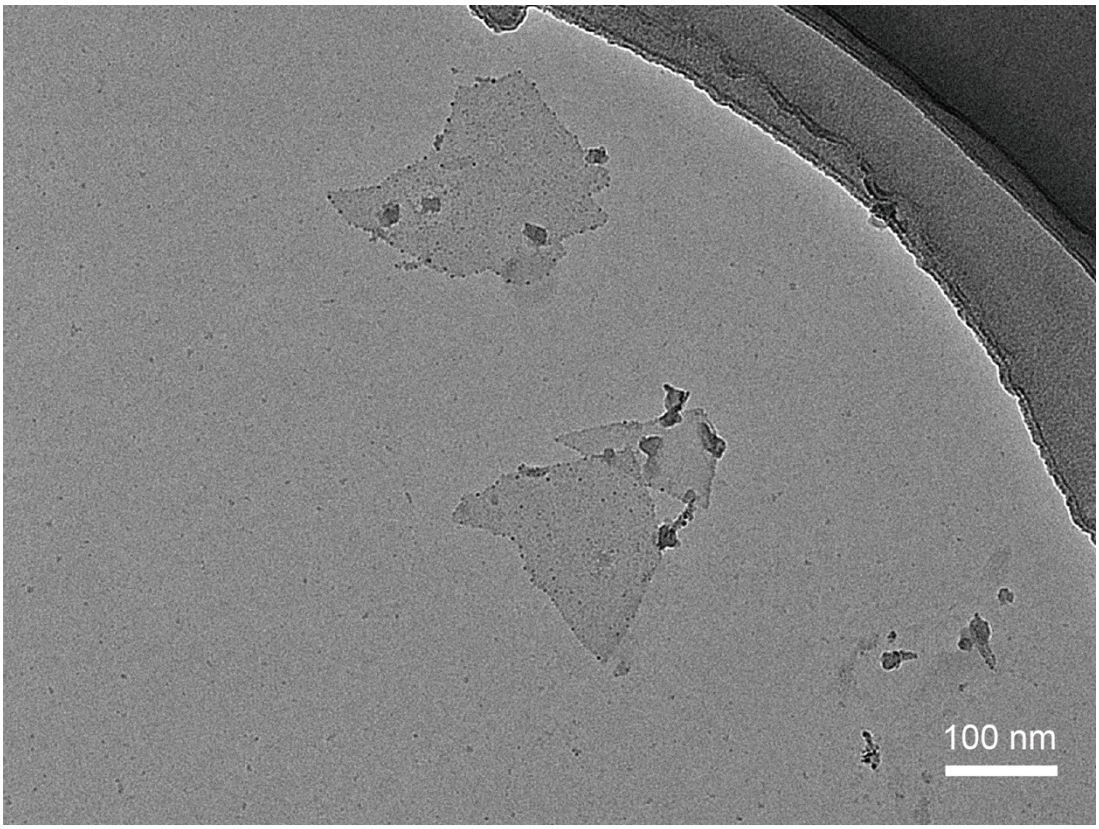

Fig. S5 TEM image of HF-$Ti_3C_2T_x$ using TMAOH as intercalation reagent

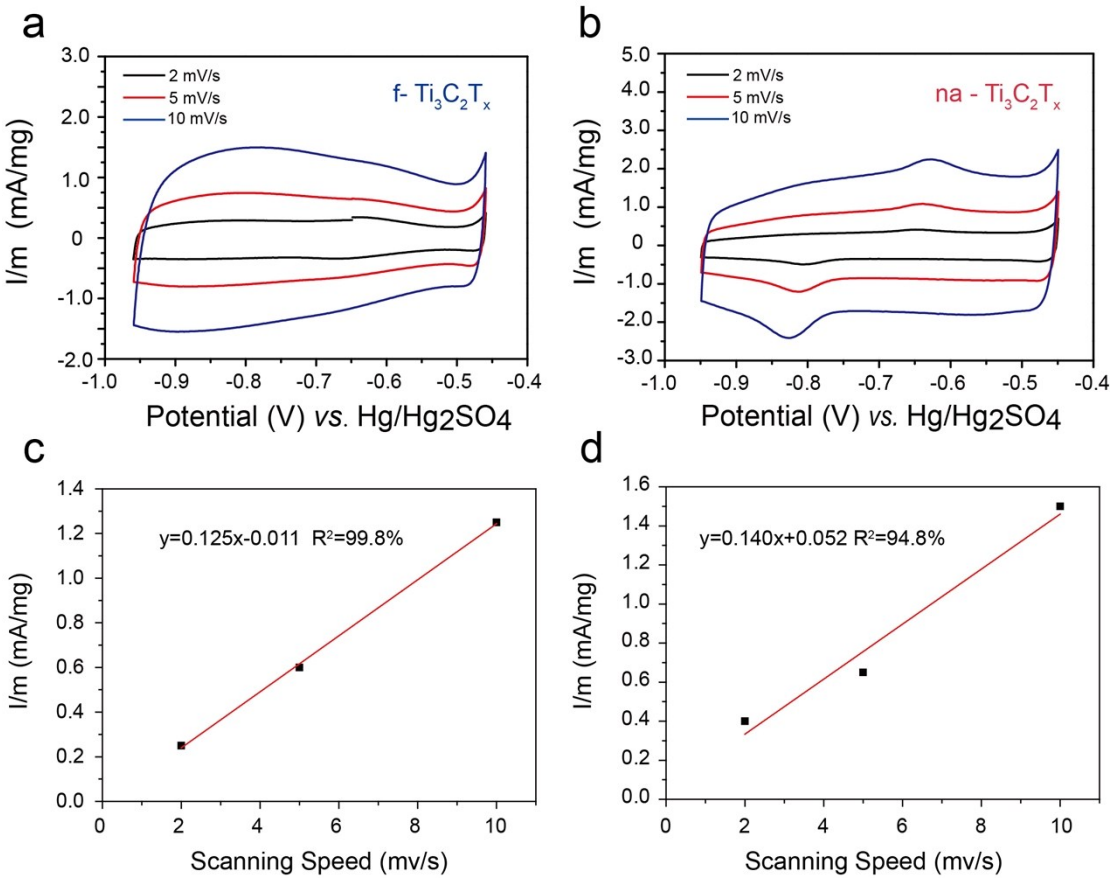

Fig. S6 (a)CVs of HF-$Ti_3C_2T_x$ and (b)NaOH-$Ti_3C_2T_x$ at 2, 5, 10 mV/s. The determined specific area of the system is taken as the slope of the linear fits to the data. (c) HF-$Ti_3C_2T_x$ and (d) NaOH-$Ti_3C_2T_x$

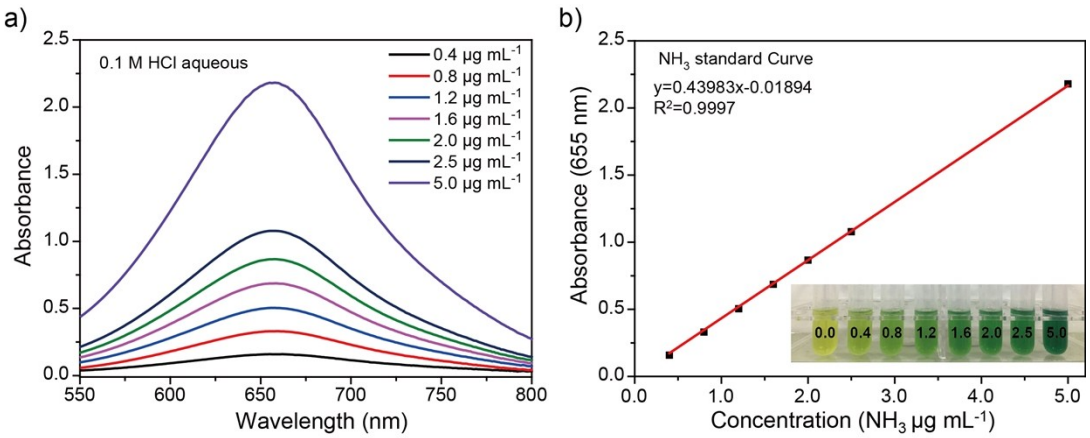

Fig. S7 Calibration of the indophenol blue method using a series of NH_4Cl standard solutions

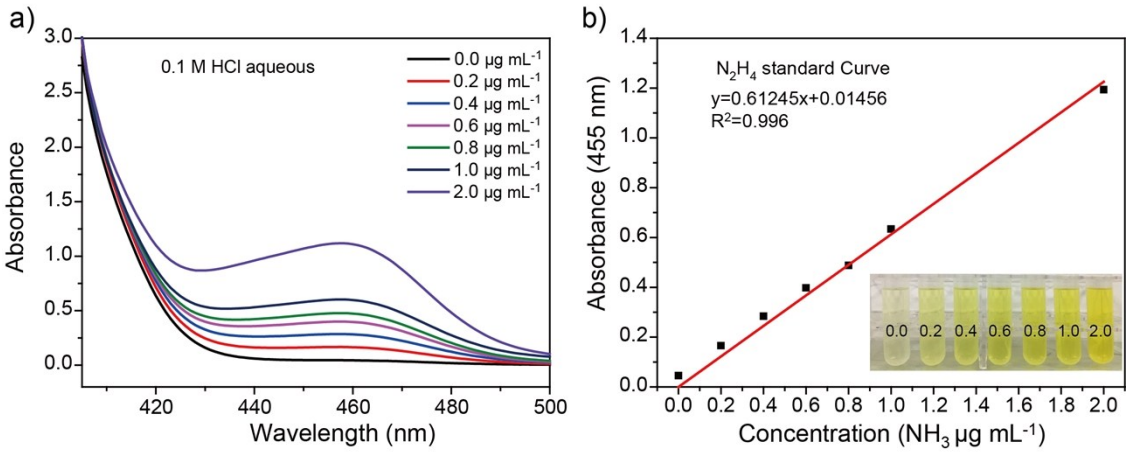

Fig. S8 Calibration of the Watt and Chrisp method using a series of N_2H_4 standard solutions

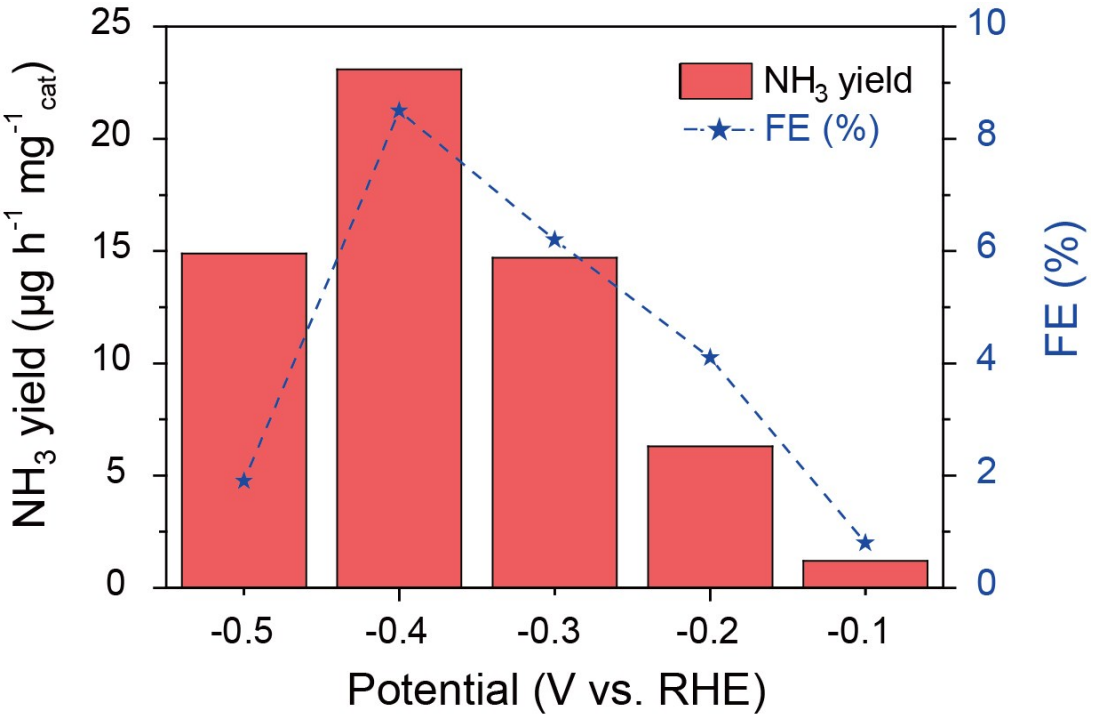

Fig. S9 NH_3 yield and Faraday efficiency of HF-$Ti_3C_2T_x$ nanosheets using TMAOH as intercalation reagent

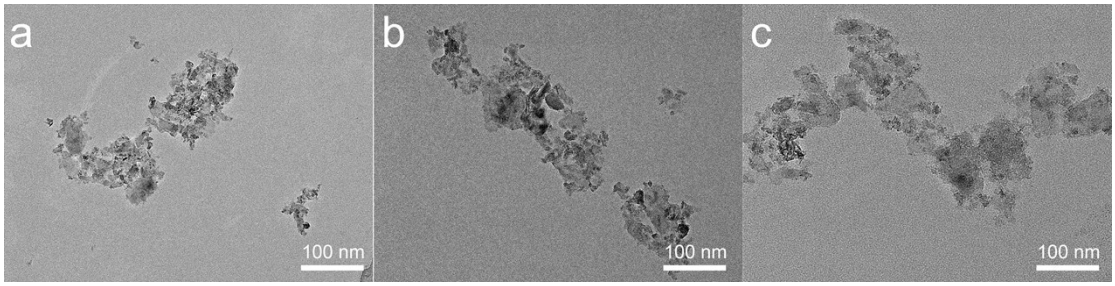

Fig. S10 TEM images of NaOH-$Ti_3C_2T_x$ nanosheets using (a) DMSO, (b) DMF and (c) Ethanol as intercalation reagents

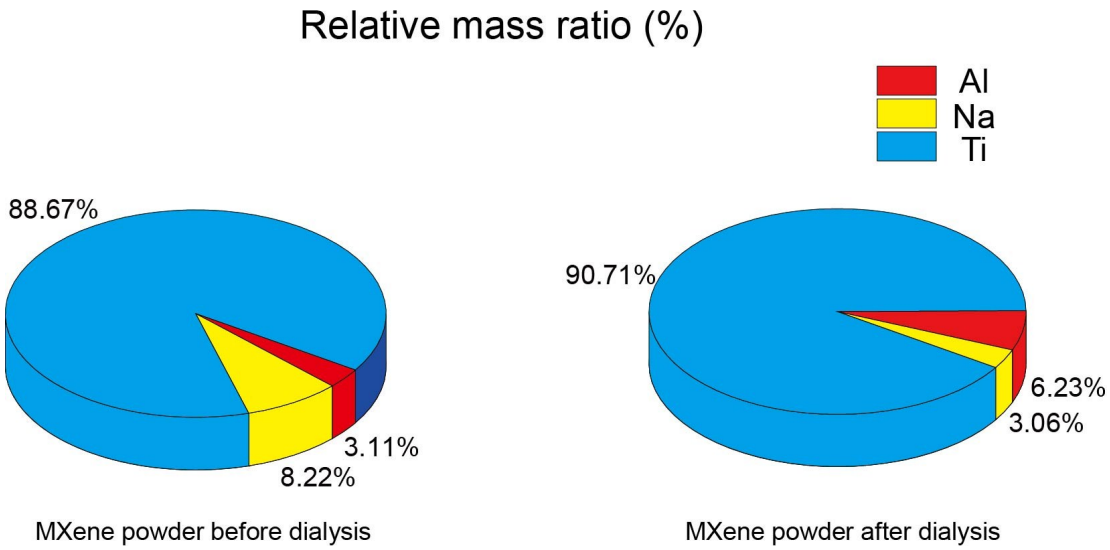

Fig. S11 ICP data of NaOH-$Ti_3C_2T_x$ powder before and after dialysis step

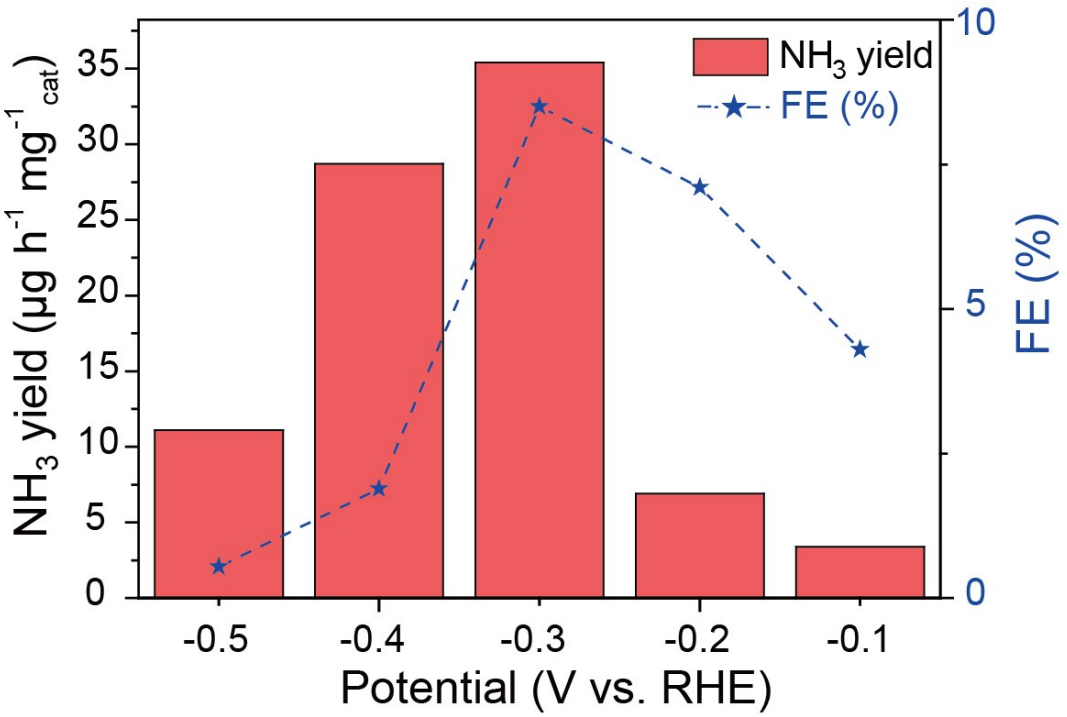

Fig. S12 NH_3 yield and Faraday efficiency of NaOH-$Ti_3C_2T_x$ nanosheets with dialysis step.

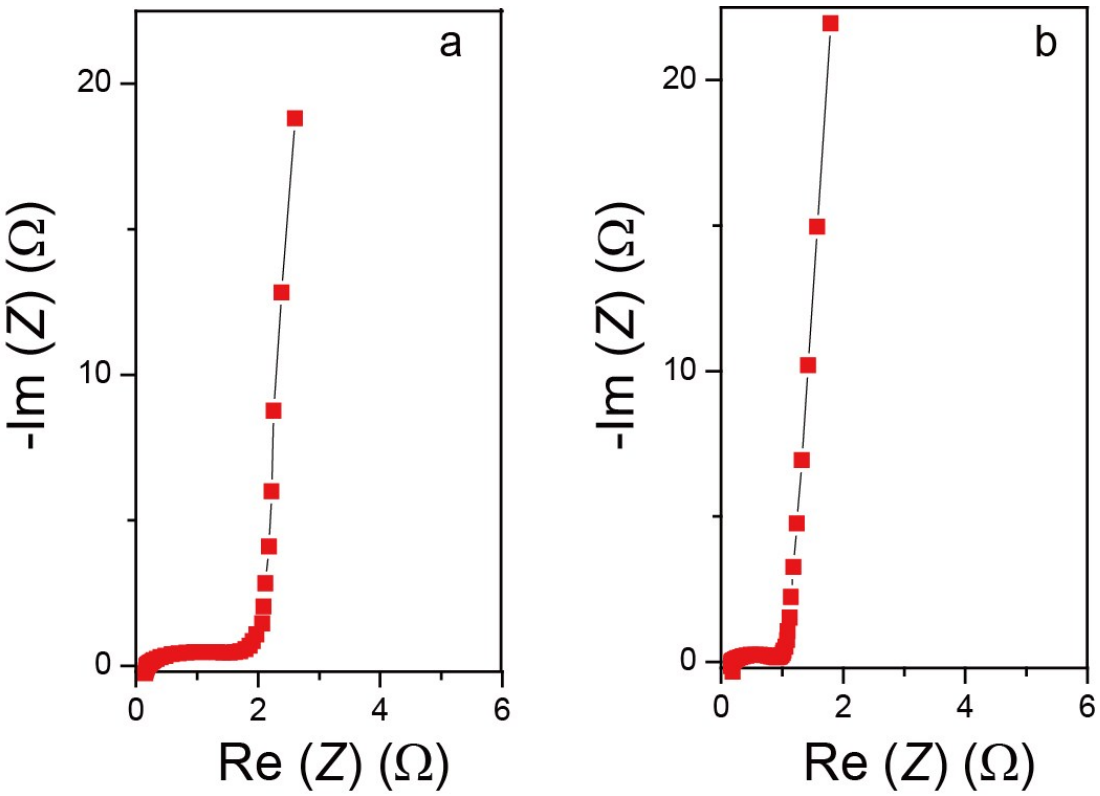

Fig. S13 EIS data (200 kHz to 10 mHz) of (a)HF-$Ti_3C_2T_x$ and (b)NaOH-$Ti_3C_2T_x$ at -0.3 V versus RHE

Reference

1. T. Li, L. Yao, Q. Liu, J. Gu, R. Luo, J. Li, X. Yan, W. Wang, P. Liu and B. Chen, *Angew. Chem. Int. Ed.*, 2018, **57**, 6115-6119.
2. M. Alhabeb, K. Maleski, B. Anasori, P. Lelyukh, L. Clark, S. Sin and Y. Gogotsi, *Chem. Mater.*, 2017, **29**, 7633-7644.
3. D. Zhu, L. Zhang, R. E. Ruther and R. J. Hamers, *Nat. Mater.*, 2013, **12**, 836-841.
4. G. W. Watt and J. D. Chrisp, *Anal. Chem.*, 1952, **24**, 2006-2008.
5. J. Zhao, L. Zhang, X.-Y. Xie, X. Li, Y. Ma, Q. Liu, W.-H. Fang, X. Shi, G. Cui and X. Sun, *J. Mater. Chem. A*, 2018, **6**, 24031-24035.
6. Y. Fang, Z. Liu, J. Han, Z. Jin, Y. Han, F. Wang, Y. Niu, Y. Wu and Y. Xu, Adv. Energy Mater., 2019, 1803406.
7. Y. Luo, G.-F. Chen, L. Ding, X. Chen, L.-X. Ding and H. Wang, Joule, 2019, **3**, 279-289.